Mechanisms for Temporal Tuning and Filtering by Postsynaptic Signaling Pathways

Upinder S. Bhalla

National Centre for Biological Sciences, Gandhi Krishi Vigyan Kendra Campus, Bangalore 560065, India

ABSTRACT   Networks of signaling pathways perform complex temporal decoding functions in diverse biological systems, including the synapse, development, and bacterial chemotaxis. This paper examines temporal filtering and tuning properties of synaptic signaling pathways as a possible substrate for emergent temporal decoding. A mass action kinetic model of 16 synaptic signaling pathways was used to dissect out the contribution of these pathways in linear cascades and when coupled to form a network. The model predicts two primary mechanisms of temporal tuning of pathways: a weighted summation of responses of pathways with different timings and the presence of biochemical feedback loop(s) with emergent dynamics. Regulatory inputs act differently on these two tuning mechanisms. In the first case, regulators act like a gain-control on pathways with different intrinsic tuning. In the case of feedback loops, the temporal properties of the loop itself are changed. These basic tuning mechanisms may underlie specialized temporal tuning functions in more complex signaling systems in biology.

INTRODUCTION

Temporal patterning is an important feature of natural stimuli to cells. Signaling and genetic networks in many cell types respond in a highly selective manner to a continuum of temporal events from the diurnal rhythm to millisecond intervals between action potentials (Barr et al., 1995; Fields et al., 1997; Markram et al., 1997; Scheper et al., 1999). These temporal computations frequently involve cellular specializations, including compact cytoskeletal structures mediating interactions between individual molecules (Levchenko et al., 2000; Lu et al., 2001; Shimizu et al., 2000), compartmentalization and local diffusion (Svoboda et al., 1996), and complex cellular machinery (Soderling and Derkach, 2000). Simple mass-action chemistry is a common denominator of these specialized cellular computing networks. This paper asks whether simple biochemical circuits can perform the fundamental temporal operations of tuning and filtering, and using a small selection of pathways seeks to identify candidate mechanisms for doing so.

Synaptic signaling is a particularly well-studied system where different temporal input patterns are converted into a wide repertoire of signaling and cellular outputs manifesting as different forms of synaptic plasticity (Abbott and Nelson, 2000; Bliss and Collingridge, 1993). A large number of signaling pathways have been implicated in these processes, and they form a relatively well-characterized network (Lisman, 1994). The sliding threshold rule (Stanton, 1996) generalizes many experiments to relate stimulus intensity (corresponding to pulse frequency and calcium elevation) and the direction of synaptic change. Stimulus intensity and

frequency are clearly a first approximation to the complex temporal patterns found in nature. There is increasing evidence to show that the direction and type of synaptic change is a rather complex function of stimulus pattern (Abbott and Nelson, 2000; Fields et al., 1997; Grover and Teyler, 1990). Further, different signaling pathways also seem to be activated in a stimulus pattern-dependent manner (Blitzer et al., 1995; Winder et al., 1999). The current paper uses mass-action simulation of a network of postsynaptic signaling pathways to investigate possible mechanisms for selectivity between different temporal patterns of stimulus.

Cellular signaling, including synaptic signaling, operates in a highly context-dependent manner. Context is provided by regulatory signaling inputs such as hormones, broadcast neurotransmitters, or genetic background (Nguyen et al., 2000). From electrical circuit theory the commonest approach to changing temporal tuning is through changing the time-courses of elements of the circuit (Horowitz and Hill, 1989). The simulations in the current paper suggest that in signaling, alternative tuning is also accomplished through up- and down-regulation of pathways, thereby changing the relative weights given to responses with different intrinsic time-courses.

The current analysis uses two kinds of stimuli to explore the range of tuning properties of pathways. These stimuli are meant to be representative of simple inputs to natural systems. The first stimulus is a single Ca^{2+} pulse of varying amplitudes and duration. The second stimulus consists of two brief Ca^{2+} pulses separated by different intervals. More complex stimuli can be constructed as composites of these basic patterns. The simulations show strong temporal tuning both at the pathway and the network level, and this tuning is a function of regulatory input. Two key mechanisms of tuning emerge: weighted summation of inputs having different time-courses and regulator-dependent shifts in response time-courses of feedback loops. Thus, rather sophisticated tuning properties emerge even from simple mass-

action approximations to relatively small signaling networks.

MATERIALS AND METHODS

Simulation methods and the network of signaling pathways were based on those previously described (Bhalla and Iyengar, 1999). Briefly, a point mass-action model of chemical kinetics was used to represent each signaling pathway based on pharmacological and test-tube experiments using purified proteins as published in the literature. Reactions of the form

$$A + B \leftrightarrow C$$

were represented as differential equations of the form

$$dA/dt = -kf[A] \times [B] + kb[C]$$

and solved using the exponential Euler method (MacGregor, 1987) using the simulator GENESIS and the chemical kinetics interface Kinetikit (Bhalla, 1998). All computations were done on PCs running Linux. Enzyme reactions were modeled using the Michaelis-Menten scheme

$$E + S \leftrightarrow E \cdot S \rightarrow P + S$$

which is equivalent to two simple reactions in sequence. Pathways were defined according to interactions defined through published experiments using pharmacological, genetic, and molecular biological techniques.

The model consisted of 16 signaling pathways including the four major kinases protein kinase C (PKC), protein kinase A (PKA), mitogen activated protein kinase (MAPK), calcium-calmodulin activated protein kinase type II (CaMKII), and their regulators (Fig. 1). Each signaling pathway was represented as several distinct chemical steps and intermediate molecular species. The expanded reaction scheme for the Ras pathway is illustrated in Fig. 1 C. A total of 148 molecular species, 84 reactions, and 65 Michaelis-Menten enzyme activities were modeled. Simulation parameters and data sources are presented in the supplementary material. Simulation software, signaling pathway models, and parameters used in the current paper have been uploaded to the DOQCS database (http://doqcs.ncbs. res.in) in accession number 16.

Inputs to the model were in the form of buffered calcium pulses of defined amplitude and duration. Calcium directly elevates the activity of PKC, phospholipase A_2 (PLA$_2$), and phospholipase C (PLC) β. It also acts through calmodulin (CaM) to activate Ras/MAPK, AC1, phosphodiesterase, CaMKII, and calcineurin (Fig. 1). Thus, calcium pulses have an effect on most pathways in the system and are useful for probing network responses. Regulatory inputs were delivered as buffered inputs in the case of ligands such as Glu and epidermal growth factor (EGF) and as elevated initial protein concentrations in the case of activated type s (stimulatory) G protein (Gs)-α.

Thresholds for turn-on of the feedback loop were calculated using an iterative bisection algorithm as follows: An initial stimulus was delivered halfway between preset minimum and maximum stimulus levels. The response of PKC was monitored. If it exceeded a predefined level (0.2 μM active PKC) 3000 s after the stimulus, the stimulus was considered to be above threshold. Stimulus amplitudes were adjusted such that each was halfway between the latest supra-threshold and sub-threshold stimulus, i.e., at the mean of the two. This process of bisection enables determination of the stimulus threshold to 1 part in 2^N, where N is the number of cycles of bisection. A similar algorithm using geometrical means rather than arithmetic means was used when the stimulus range was large.

The mechanisms of tuning and its regulation were investigated for continuous stimuli at different amplitudes and durations, and for pulse stimuli of 1 s separated by different intervals. For each stimulus, a variety of stimulus intensities and a range of regulatory conditions were examined to characterize the response time-courses. The contributions of different
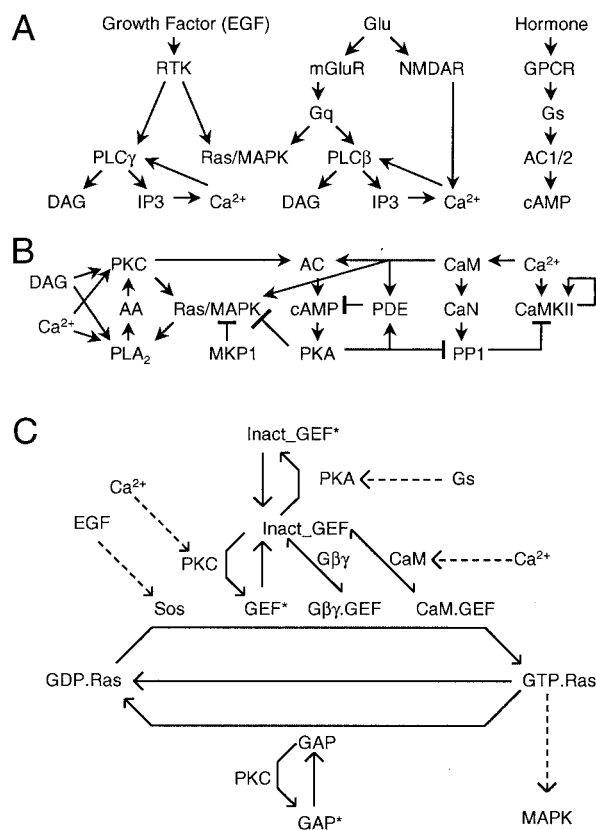

FIGURE 1 Block diagram of signaling network. Excitatory interactions are indicated with arrows, inhibitory interactions with T-junctions. Each block in the diagram is modeled as several reactions. (A) Inputs and immediate downstream pathways. Calcium feeds back onto PLCβ and γ, but in this model calcium levels were held fixed so the release of calcium by inositol trisphosphate was not modeled. (B) Four major kinases and their regulators. Some molecule names are repeated in the diagram for clarity, but in the model each molecule is represented uniquely. Calcium stimulates PKC and PLA2 directly, and several additional pathways through CaM. (C) Reaction scheme for one of the signaling blocks, the Ras pathway. Indirect inputs and outputs are represented by dotted lines. Chemical reactions are represented by straight lines with arrows and enzymatic reactions by arrows with a bend and the enzyme at the bend. Several molecules act as guanine nucleotide exchange factors (GEFs) for Ras, and these all represented along the reaction converting GDP.Ras to GTP.Ras. Other blocks in the model are implemented at a similar level of chemical detail and are shown in full at http://doqcs.ncbs.res.in, accession 16.

mechanisms for temporal tuning were probed by modeling a variety of blockage and stimulation experiments on the synaptic signaling network.

RESULTS

Response time-courses of pathways

First, the basic tuning properties of pathways in the network were characterized by applying a Ca^{2+} input stimulus of constant total Ca^{2+} influx over baseline, but different durations from 1 to 900 s (Fig. 2). Thus, brief stimuli had high calcium levels, which strongly activated some pathways such as CaMKII and PKA, which are downstream of CaM.
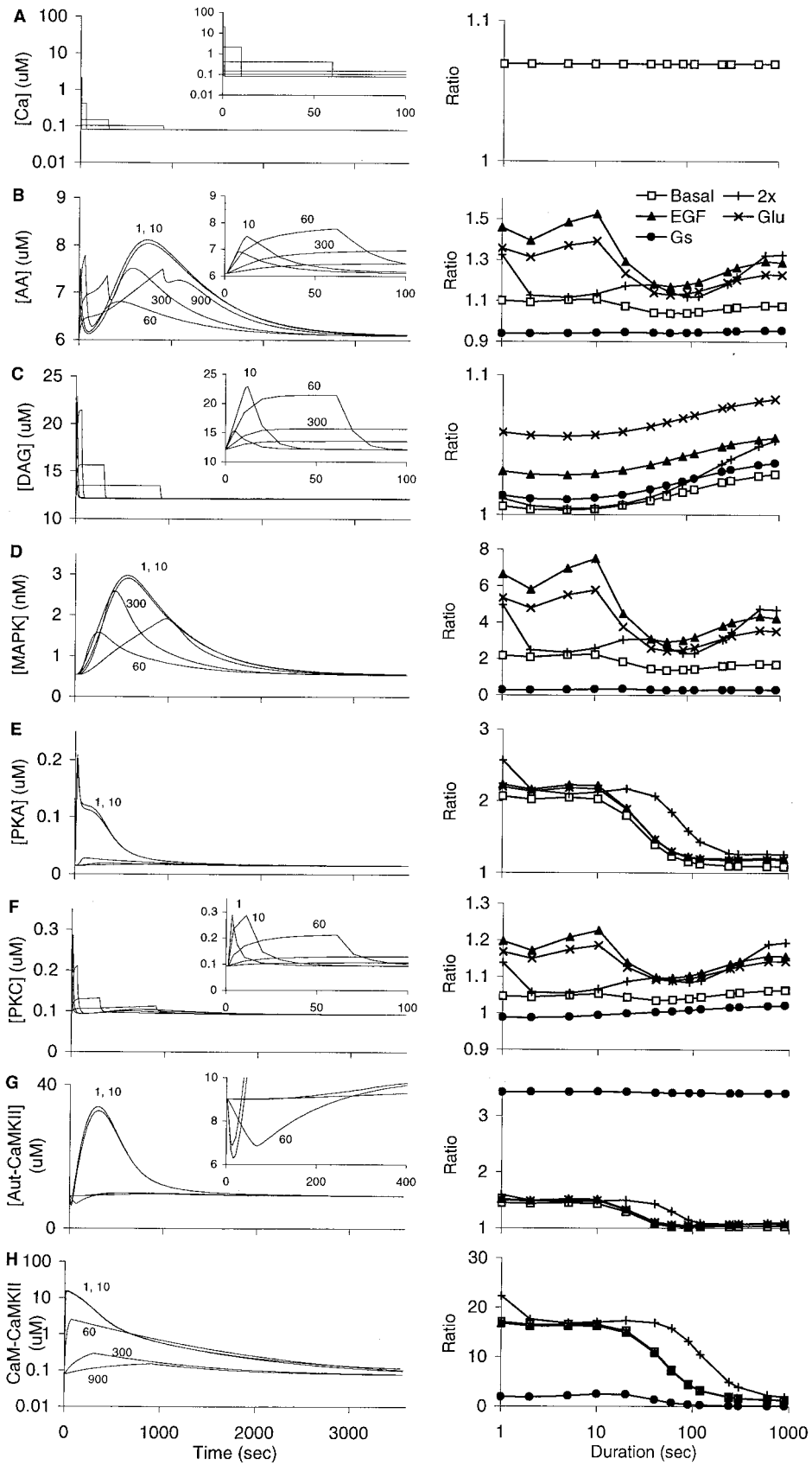
Prolonged stimuli had lower calcium levels, but if the affinity for Ca^{2+} was sufficiently strong this could result in activation for a longer period, e.g., $PLC\beta$ as measured by diacylglycerol (DAG) production. Even with this simple steady Ca^{2+} pulse, most pathways (with the exception of $PLC\beta$/DAG) exhibited quite complex temporal patterns of response. Based on the signaling network diagram, it seemed likely that these complex patterns were due to summation of inputs of different time-courses. This is considered in detail later in the paper.

As a measure of total activity of the pathway over the entire time course of its response, the ratio of instantaneous activity to basal activity was averaged over a 3600-s period after the stimulus onset. This quantity is referred to as the activation ratio. The activation ratio is plotted as a function of stimulus duration (Fig. 2, right column; basal curves indicated by open squares). Calcium, by design, has a uniform ratio (Fig. 2 *A*). The remaining molecules can be broadly categorized into three groups: DAG activity rises slightly with stimulus duration; PKA and CaMKII activity declines with stimulus duration, and the remainder (arachidonic acid (AA), MAPK, and PKC) have a biphasic response that is higher for brief and prolonged stimuli but lower for intermediate durations. Thus, the responses are tuned to different stimulus durations. The tuning factor, that is, the maximum by the minimum activation ratio, is large (10 fold) for CaM-CaMKII and moderately large (over twofold) for MAPK and PKA. Other pathways also exhibited some tuning, but high baseline activity lowered the tuning factor.

It was tested whether the basal tuning patterns were consistent when Ca influx was doubled (crosses in Fig. 2, right column). Interestingly, the tuning patterns changed both in terms of amplitude and timing. AA, MAPK, and PKC, which are tightly coupled, all responded differently from the basal stimulus. There was an initial large response for the 1-s stimulus, then a drop, followed by a slow

increase with increasing stimulus duration. The activation ratio curve for PKA and both forms of CaMKII was similar to the basal curve, but it was shifted to threefold longer stimulus durations. This shift can be explained by the highly cooperative activation of CaM by Ca^{2+}, which gives rise to a sharp Ca^{2+} dependence. As long as Ca^{2+} levels are greater than the threshold for CaM activation, the downstream pathways PKA and CaMKII will be activated. Therefore, at higher total Ca^{2+} flux, the duration of activation is extended.

How does this tuning depend on regulatory inputs? The AA, MAPK, and PKC curves again show tightly coupled responses to regulators (Fig. 2, right column). EGF and glutamate inputs both amplify the responses considerably, but the shape is similar to the basal response. Gs causes a sharp decline in the responses because PKA inhibits the MAPK pathway. Interestingly, PKC shows a small but distinct increase rise in response with increasing duration even in the presence of Gs. PKA is directly downstream of Gs, and its activity is saturated with the 5-nM Gs stimulus (data not shown). This effect cascades onto the autonomous CaMKII activity because PKA inhibits protein phosphatase 1 (PP1), which reverses autophosphorylation and autonomy of CaMKII. The large increase in autophosphorylated CaMKII reduces the pool of native CaMKII, and hence Gs reduces the CaM-CaMKII response.

An interesting signaling motif, which integrates multiple inputs, is the feedback loop (Bhalla and Iyengar, 1999; Ferrell and Machleder, 1998; Roberson and Sweatt, 1999). The current model includes both a CaMKII autophosphorylation loop (Hanson et al., 1994) and a MAPK-PLA_2-PKC loop. Each of these loops receives inputs from Ca^{2+} as well as regulatory signals. CaMKII is activated by Ca_4.CaM. It is also regulated by the Gs pathway through adenylyl cyclase (AC), cyclic adenosine monophosphate (cAMP), PKA, and PP1 (Fig. 1). The MAPK-PLA_2-PKC feedback loop receives multiple inputs from calcium as well as regulators.

FIGURE 2 Responses of representative enzymes to calcium pulses of different duration but the same total flux (20 μM·s). (*Left column*) Time course of response. (*Right column*) Ratio of total activity to baseline as a function of stimulus duration and different regulatory conditions. This column can be interpreted as a measure of tuning to different stimulus durations. $\square$, Basal conditions with no regulatory inputs and 20 μM·s calcium flux; +, basal conditions at 40 μM·s calcium flux; $\blacktriangle$, 20 μM·s Ca, 0.2 nM EGF; $\times$, 20 μM·s Ca, 0.1 nM Glu; $\bullet$, 20 μM·s Ca, 5 nM Gs. (*A*) Calcium. Inset shows Ca^{2+} levels at a finer time-scale. (*B*) AA, as a measure of PLA_2 activity. Inset shows AA activity at finer time-scales. The response time course is biphasic with a sharp initial rise that terminates as soon as Ca^{2+} is removed, and then a slower response ~600 s after the first. In the right column, the ratio of averaged activity for AA is also biphasic and has a minimum at a duration of ~100 s. Glutamate and EGF regulatory inputs increase the sharpness of tuning as compared with the basal or Gs-stimulated conditions. Stronger stimulus (+) gives a complex tuning curve that differs from the others. Gs suppresses the output and the tuning is nearly flat. (*C*) DAG, as a measure of $PLC\beta$ activity. Inset shows DAG levels at a finer time-scale. This response follows the Ca^{2+} time course very closely. The ratio of averaged activity (*right column*) is very close to one for all stimulus durations and regulators, but there is a slight change in averaged activity depending on regulator. (*D*) MAPK activity, measured as levels of the active kinase. MAPK is upstream of PLA_2, note similarity of MAPK response to second phase of PLA_2 response, and also similarity of activity ratio plots. (*E*) PKA has a distinct shoulder in its response amplitude for 1- to 10-s stimuli. PKA responses drop sharply for longer duration stimuli because Ca^{2+} levels fall below the CaM binding affinity. This is seen both in the response amplitude and also in the activation ratio curve. Regulators do not have much effect but a stronger stimulus shifts the activation ratio curve over to the right. (*F*) PKC activity follows the Ca^{2+} stimulus closely, but there is a small and slow delayed response at ~600 s. The PKC activation ratio remains quite close to unity but is otherwise similar to that for MAPK and AA. (*G*) Autonomous CaMKII undergoes a brief initial dip followed by a very strong elevation for Ca^{2+} durations under 10 s. At longer durations Ca^{2+} levels are too low to activate CaM. The initial dip is due to CaM trapping during the period when Ca^{2+} is present. The activation ratio curve is similar to but smaller than that for PKA. (*H*) CaM-bound CaMKII is stimulated by the initial Ca^{2+} influx and then declines steadily. Like PKA, CaM binding thresholds for Ca^{2+} leads to a drop in activation ratio at long stimulus durations.

The MAPK cascade receives input through Ras, which is stimulated by many signals including $Ca_4.CaM$. PLA_2 and PKC are both directly activated by Ca^{2+}. These interactions are outlined in Fig. 1. The MAPK-PLA_2-PKC feedback loop is bistable under the conditions of this model (Bhalla and Iyengar, 2001), that is, the loop has two stable states of different activities. In the low stable state the activities of MAPK, PLA_2, and PKC are all at basal levels for the respective enzymes. In the high stable state, each of the loop enzymes is in a state of high activity. Bistable feedback systems have the useful property of sharp thresholding (Thron, 1997). Threshold in this model is defined as the level of calcium stimulus just sufficient to take the system from the stable state of basal activity to the stable state of high activity. As discussed in Materials and Methods, in this calculation the activity of PKC was used as a measure of the loop activity, but any of the loop enzymes could have been used. Although each enzyme has individual levels of high and low activity, the threshold and lower and upper stable states are properties of the feedback loop as a whole. Crossing this threshold is an all-or-none event and thus acts as a simple readout of many inputs impinging on the feedback loop. Therefore, the threshold of the feedback loop for Ca^{2+} flux was used as an integrated measure of temporal tuning of the network as a whole (Fig. 3 A). The same set of inputs of varying duration were applied, and the threshold was calculated in terms of the total Ca^{2+} flux. Under all regulatory conditions, the threshold started out rather low for short strong stimuli. At intermediate stimulus durations the thresholds were high, and then there was a decline again for long stimulus durations. As expected, this tuning curve is qualitatively the inverse of that seen in Fig. 2 for the activation ratio at different durations. Regulators significantly affected tuning. The highest thresholds were for Gs stimulation and the lowest for Glu stimulation, which again could be predicted from the results in Fig. 2. Surprisingly, regulatory inputs shift the duration at which the threshold is highest. This shift spans nearly an order of magnitude from 5 s for Glu to 40 s for Gs. This contrasts with the situation for activation ratio tuning in Fig. 2, B and D, where the minimum activation ratio was at ~100 s for all regulatory inputs. Another surprising observation is that the largest tuning factor for thresholds occurs for Gs regulation and the lowest for Glu input. This reverses the situation from Fig. 2, B, D, and F where the tuning was quite weak for Gs and strong for Glu regulation. Clearly the integrated response of the bistable feedback loop is a complex function of the individual pathway inputs.

As another way of visualizing the tuning to stimulus duration, the threshold stimulus amplitude is plotted as a function of stimulus duration (Fig. 3 B). Here it appears that the required Ca^{2+} amplitude remains nearly constant (and very large) for a range of brief stimulus durations and then drops sharply and commences a nearly linear decline with
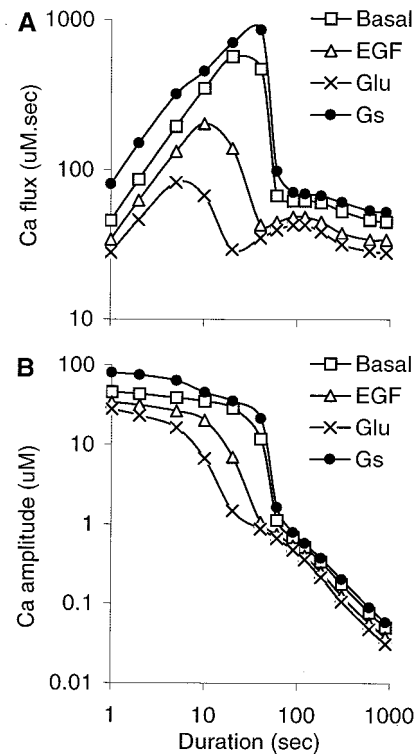

FIGURE 3 Threshold plots for the MAPK-PLA_2-PKC feedback loop for different stimulus durations. Threshold is the stimulus level required to switch the feedback loop from the basal to the active state. A high threshold means that the stimulus is ineffective in activating the loop, whereas a low threshold means that the loop is activated even for relatively low values of the stimulus. (A) Threshold Ca^{2+} flux at different stimulus durations. There is a steady increase followed by a sharp drop in required flux for durations of over 100 s. Regulators shift both the peak threshold and the stimulus duration at which the threshold drops. Gs (1 nM) acts in an inhibitory manner, raising thresholds. EGF and Glu (0.1 nM each) act in an excitatory manner. Both lower the threshold and reduce the duration for the threshold drop. (B) Threshold Ca^{2+} amplitude at different stimulus durations. These plots are related to those in A by the formula flux = amplitude × duration. The initial threshold Ca^{2+} amplitude remains almost constant and then drops rapidly before commencing a nearly linear decline with increasing duration. Again the threshold and the stimulus duration for the threshold drop are functions of regulatory inputs.

increasing stimulus duration. Regulators change the duration at which the sharp decline occurs.

Interval tuning

Repetitive stimuli are a common form of natural stimulus patterning. This was modeled using two 1-s Ca^{2+} pulses separated by different intervals (Fig. 4). The 1-s Ca^{2+} input has a time course shorter than any of the signaling pathways, and thus the responses of the pathways are not a function of its duration or shape, only of the Ca^{2+} influx. This is a way of determining nonlinearity in summation of temporal responses. The response to the second pulse could
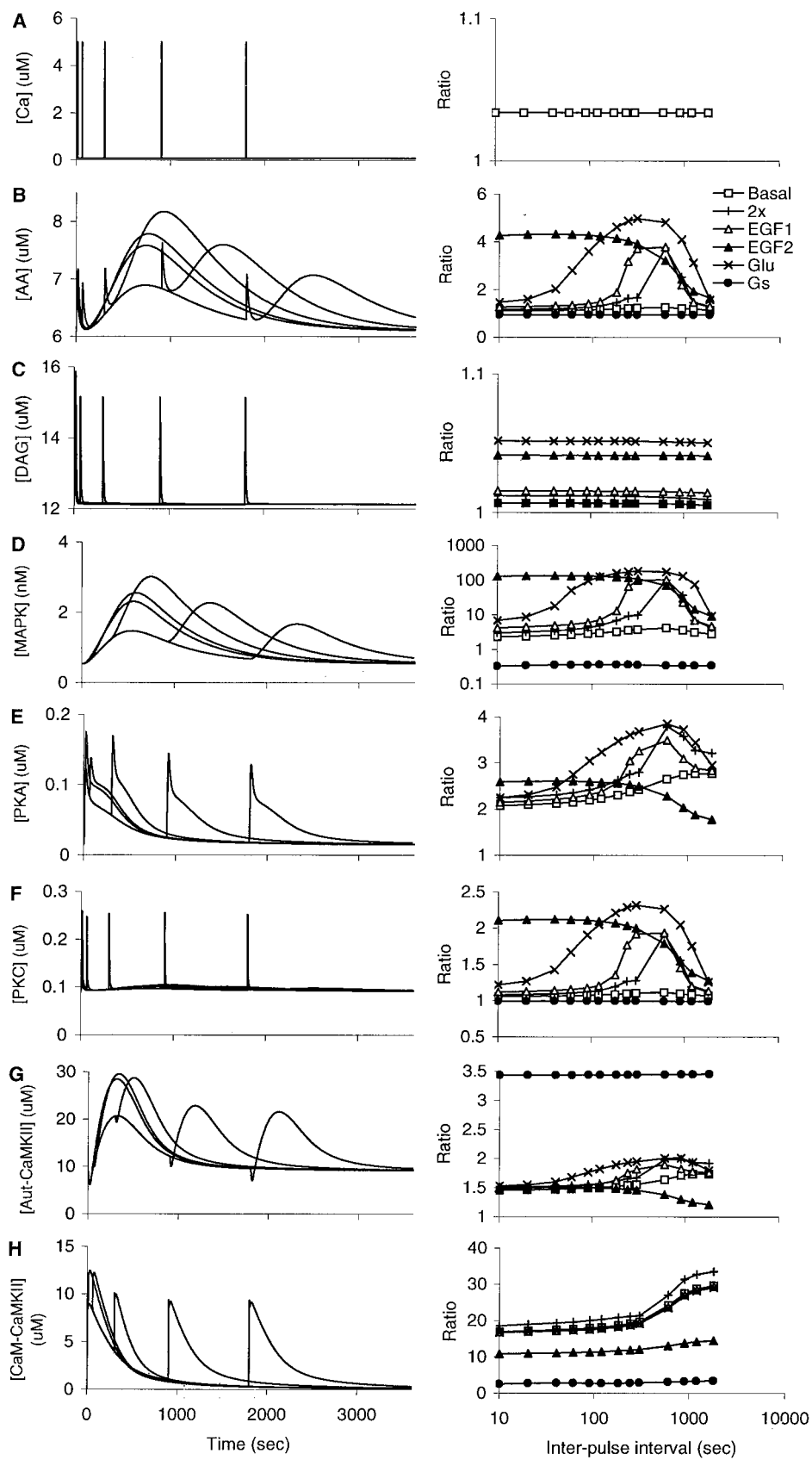
also be regarded as a measure of the history dependence of the signaling system.

Three responses had a simple unimodal time course: PLCβ (as measured by DAG), MAPK, and CaM-CaMKII (Fig. 4, left column). AA has a sharp initial response to the calcium transient through direct activation of PLA_2 by Ca^{2+}, and a slower response, which closely follows the MAPK activation. PKC has a very brief and sharp direct response to Ca^{2+} and a much smaller and slower response to AA. PKA has a "shoulder" in its response curve where the initial CaM elevation declines and thus CaM-phosphodiesterase ceases to hydrolyze cAMP. Autonomous CaMKII has an initial dip because of calmodulin trapping after the initial Ca^{2+} elevation (Meyer et al., 1992). Subsequently the autophosphorylation builds up at a slower timescale. Visual inspection of the responses suggests that the summation of the second pulse is nearly linear in most cases except MAPK and AA, where the peak amplitudes are distinctly supralinear.

A more quantitative measure of summation is to take the activation ratio, defined as the ratio of instantaneous response to baseline averaged over the entire response duration (Fig. 4, right column, square symbols for basal responses). The Ca^{2+} ratio is uniform as expected. AA, MAPK, and PKC, which are tightly coupled, show a small amount of basal tuning for interpulse intervals around 300 to 600 s. PLCβ/DAG shows no tuning. The basal responses for PKA and the two states of CaMKII are lower at short intervals than at intervals longer than their intrinsic time-courses. This implies that when responses to successive stimuli overlap, the total response is smaller than when the two stimuli are well separated in time. Thus, the responses of these pathways sum sublinearly.

Increased stimulus amplitudes (+ symbols, Fig. 4, right column) had large effects on the AA/MAPK/PKC combination. The response at an interval of 600 s was much larger than at other times, as the feedback loop crossed threshold for this stimulus interval. PKA activation ratio also jumped at 600-s stimulus intervals, as a downstream effect of PKC→AC2→AMP→PKA. The two CaMKII forms had modest increases in activation ratio.

Regulatory inputs altered temporal tuning in a variety of ways. A striking example of different tuning effects is seen for two different combinations of EGF and stimulus amplitude (10 μM Ca and 0.1 nM EGF, open triangles; 2 μM Ca and 0.5nM EGF, filled triangles in Fig. 4, right column). The AA/MAPK/PKC combination responds strongly to a range of intervals between 180 and 600 s for the EGF1 stimulus (open triangles). In the case of EGF2 (filled triangles) the response is high until 600-s interval, and then it drops. Another case of contrasting tuning is seen for PKA, where the response to EGF2 stimulus (filled triangles) is almost the exact inverse of the baseline response tuning (open squares). The glutamate stimulus (10 μM Ca and 0.1 nM Glu) increases the amplitude of the responses and broadens the range of intervals to which the system responds in all cases except DAG and CaM-CaMKII. The Gs stimulus appears to nearly null out any interval tuning, and it suppresses the response amplitudes except for PKA and autonomous CaMKII. None of the regulators affected DAG tuning and effects on its activation levels were small.

The feedback loop threshold calculation was used as a measure of integrated network responses to different interpulse intervals and regulators (Fig. 5). The threshold declines steadily to a minimum at an interval of ~600 s and then rises again. Regulators strongly affect thresholds. The highest threshold is in the presence of Gs and the lowest in the presence of EGF as was the case for duration thresholds. Unlike the case for duration, regulators do not appear to shift the time of the lowest threshold. Overall, the network appears to be tuned to an interpulse interval of ~600 s.

Weighted combination of inputs

The tuning properties seen above emerge from a network of several pathways. I wished to address the mechanistic basis of this tuning at the single-pathway level. From the responses of the pathways in Figs. 2 and 4, it appeared likely that complex responses might arise from summation of inputs from multiple pathways, each with different time-courses. I therefore considered three illustrative pathways,

FIGURE 4 Responses of representative enzymes to 1-s Ca^{2+} pulses, separated by different intervals. Left column is the time-courses of responses to 5-μM Ca^{2+} pulses. Right column is the ratio of averaged activity to basal activity, which can be interpreted as a tuning curve for different stimulus intervals. □, Tuning curves for the basal signaling network stimulated at 10 μM Ca without any applied regulators; +, Basal conditions with a 20-μM Ca stimulus; △, 10 μM Ca stimulus and steady 0.1 nM EGF; ▲, 2 μM Ca stimulus and steady 0.5 nM EGF; ×, 10 μM Ca and 0.1 nM steady Glu. ●, 10 μM Ca and steady 5 nM Gs. (A) Ca^{2+} stimulus. (B) AA as a measure of PLA_2 activity. Strong stimuli and excitatory regulators (Glu and EGF) cause the MAPK-PLA_2-PKC loop to switch to a state of high activity, and thus high activation ratios are observed for some stimulus intervals for which the system is well tuned. The tuning depends on regulatory input as well as stimulus strength. (C) DAG as a measure of PLCβ activity. The response (*left column*) is very brief and follows the Ca^{2+} stimulus almost perfectly. Activation ratio (*right column*) is nearly flat with respect to stimulus interval but regulators do cause small differences in activation ratio. (D) MAPK activity matches the slow phase of AA activity very closely. In the right column the ratio of averaged activity is also very similar in shape to AA, but the fold tuning is quite large. MAPK is upstream of PLA_2. (E) PKA activity. Basal activation ratio increases at larger intervals. Regulatory effects are superimposed on this due to the input from PKC→AC→AMP. The Gs regulator gives rise to very high, Ca-stimulus-independent PKA activity with an activation ratio of ~38 (data not shown.) (F) PKC follows the Ca^{2+} response closely, but the second pulse rides on the slow second phase of the PKC response and is consequently higher at an interval of 600 s. Activation ratios act similarly to AA and MAPK. (G) Autonomous CaMKII activation. The activation ratio follows that of PKA. (H) CaM-CaMKII activation. Regulators have relatively little tuning effect, but they shift the activation ratio up (EGF and Glu) or down (Gs). The activation ratio rises with longer stimulus intervals.
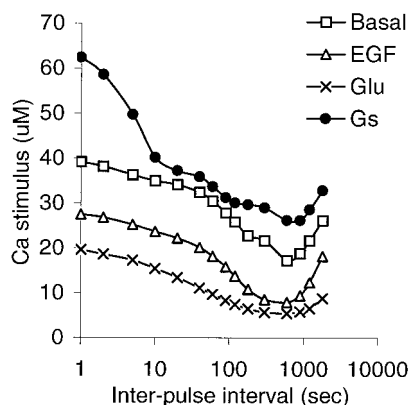
FIGURE 5 Ca^{2+} stimulus threshold for turning on the feedback loop, as a function of stimulus interval. The system is most sensitive at intervals of 300 to 600 s. This tuning occurs for all regulatory conditions, although the thresholds shift up and down.

PKA, PKC, and PLA_2 (as measured by AA production) to dissect out their responses to different inputs. Fig. 6 *A* illustrates the responses of PKA to a 1-s Ca^{2+} pulse. Ca^{2+} activates PKA through two signaling sequences: $Ca^{2+} \rightarrow CaM \rightarrow AC1/8 \rightarrow cAMP \rightarrow PKA$ and $Ca^{2+} \rightarrow PKC \rightarrow AC2 \rightarrow cAMP$. It seemed likely that the initial sharp PKA transient lasting less than 1 min might be due to the rapid Ca^{2+}-dependent elevation of PKC activity, and the slower "shoulder" might be due to the CaM pathway. This was tested by buffering either PKC or Ca4.CaM to basal levels (Fig. 6, *B* and *C*,

respectively). Contrary to the initial expectation, almost the entire response to a brief Ca^{2+} pulse was due to the CaM pathway. The efficacy of the PKC input was demonstrated by elevating PKC activity using a steady input through the metabotropic glutamate receptor (mGluR)$\rightarrow$DAG$\rightarrow$PKC pathway (Fig. 6 *D*). This elevates steady PKA activity by a factor of two but has little effect on the initial transient or shoulder in the PKA response. Overall, it appears that PKA responds rapidly to Ca^{2+} through the CaM pathway, but its response to PKC behaves like a low-pass filter. The net response of PKA is a sum of both these inputs.

I next examined PKC and PLA_2 responses to the same 1-s Ca^{2+} stimulus. In these simulations PKC has a large, transient response to Ca^{2+} stimulus through direct activation, and a much lower amplitude but broader response around 600 s following the stimulus. PLA_2, as measured by AA production, also has a transient response followed by a distinct slow peak around 600 s (Fig. 7 *A*, *i* and *ii*). I first tested whether the slower activation of PKC is due to its activation by AA. When AA was buffered to baseline, the PKC response was confined to the initial rapid transient (Fig. 7 *B*). Conversely, when the Ca^{2+} input to PKC was held at baseline and Ca^{2+} inputs to PLA_2 were enabled, the PKC initial transient was abolished and the slow response was reinstated (Fig. 7 *C*). This simulation also indicates that the contribution of the $Ca^{2+} \rightarrow PLC\beta \rightarrow DAG \rightarrow PKC$ pathway is very small. Thus, the biphasic PKC response is a composite of its direct activation by PLA_2 and direct activation by Ca^{2+}.
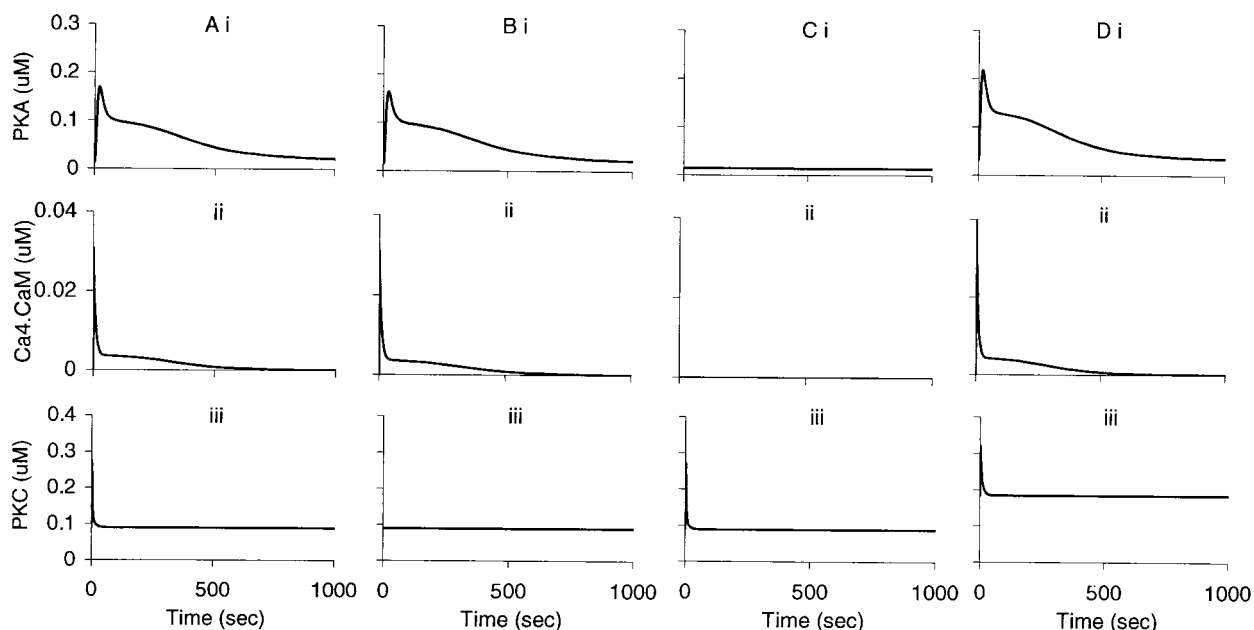

FIGURE 6 PKA responses dissected into upstream activators of AC1 and AC2 (Ca_4.CaM and PKC, respectively). The AA input to PKC has been buffered so that the PKC response only has an initial Ca^{2+} mediated phase. (*A*) Basal level responses of PKA (*i*), Ca_4.CaM (*ii*), and PKC (*iii*) to a 1-s, 10 μM Ca^{2+} stimulus. (*B*) PKC buffered to baseline. The PKA response is nearly unchanged. (*C*) Ca_4.CaM buffered to baseline. The PKA response to PKA is minimal. (*D*) Elevation of PKC basal activity. Although the transient response of PKA is hardly affected, its baseline has been raised by a factor of two. Thus, PKA filters out the rapid PKC inputs but does respond to brief Ca_4.CaM inputs and also to prolonged PKC inputs.
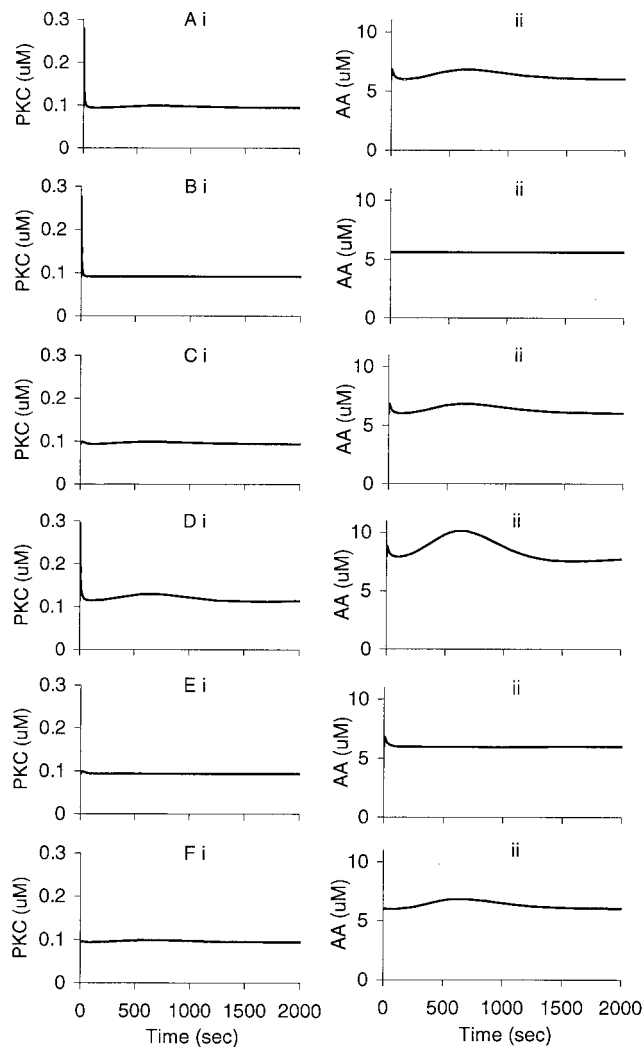
FIGURE 7 PKC and AA responses dissected in terms of upstream activators. The feedback from PKC to MAPK has been blocked for these simulations so that the responses are not complicated by feedback. (*Left column*) PKC. (*Right column*) AA, as a measure of PLA$_2$ activity. (*A*) Basal level responses of PKC and AA to a 1-s, 10 μM Ca^{2+} stimulus. Both PKC and AA exhibit an initial Ca^{2+}-stimulated transient, followed by a slower response. (*B*) AA is buffered to its resting level of 5.6 μM. PKC response is confined to the initial direct activation by Ca^{2+}. (*C*) Direct Ca^{2+} input to PKC is held at baseline (80 nM). The initial Ca^{2+}-stimulated transient is lost, but the slower late phase of response remains. In combination with the result from *B*, this suggests that the slow phase of the PKC response is due to AA stimulation. (*D*) AA activity elevated through steady EGF stimulation of the MAPK pathway. MAPK then phosphorylates and activates PLA$_2$. The time course of the AA response is nearly unchanged but the baseline and the amplitude of the peak both increase. The PKC initial response is not affected, but the late phase of PKC response is considerably magnified. (*E*) Dissection of components of AA response. The direct stimulation of PKC by Ca^{2+} is blocked, and the stimulation of MAPK by Ca$_4$.CaM is blocked. The remaining small transient in the AA response is due to direct Ca^{2+} stimulation of PLA$_2$. The PKC response is negligibly small. (*F*) Confirmation of the Ca^{2+}→CaM→MAPK→PLA2→AA→PKC pathway for slow activation of PLA$_2$ and PKC. The direct Ca^{2+} activation of PKC and PLA2 is blocked in these simulations. Only the late phase of both responses is observed.

How could a pathway switch from one time course of response to another? One mechanism could be to alter the weights of inputs having different time-courses. This was modeled by raising activation in the PLA$_2$ pathway through steady EGF input: EGF→EGFR→Sos→Ras→MAPK→PLA$_2$. The AA response, as expected, was elevated and magnified by the MAPK input, but its time course was not changed. The slow phase of the PKC response was considerably magnified (Fig. 7 *D*).

The contributions to the AA response were also investigated. Again, it seemed plausible that the initial sharp response of AA was due to direct Ca^{2+} activation of PLA$_2$, and the slower long-lasting response due to the Ca^{2+}→CaM→Ras→MAPK pathway. This was confirmed by first blocking the action of CaM on Ras (Fig. 7 *E*) and then reinstating CaM→Ras while blocking the direct action of Ca^{2+} on PLA$_2$ (Fig. 7 *F*). Thus, PLA$_2$ itself is a locus for weighted summation of inputs having different time-courses.

Tuning by feedback loops

By analogy with electrical circuits, feedback in chemical circuits is a likely site of temporal tuning and filtering (Horowitz and Hill, 1989). Both the MAPK-PLA$_2$-PKC and CaMKII autophosphorylation loops were tested for the time course of their response to a 1-s Ca^{2+} pulse under various regulatory conditions. I first tested the response of the MAPK- PLA$_2$-PKC feedback loop by applying Ca^{2+} stimuli of 1, 2, 5, 10, and 20 μM for 1 s. Although all these stimuli are well below the threshold for activation of the feedback loop ($\sim$50 μM from Fig. 3), there is a shift in the time of peak response (Fig. 8 *A*). Application of EGF increases the response amplitude (Fig. 8 *B*). Glu input affects both response amplitude and time course, especially of decay following the stimulus (Fig. 8 *C*). To see if the shift in time course was a consistent outcome of response amplitude, Gs was applied to lower MAPK activity through the inhibitory action of PKA on Ras (Fig. 8 *D*). Consistent with the trend, the time course was indeed reduced as the amplitude diminished. These effects are summarized in Fig. 8 *E*. The MAPK-PKC feedback loop response time course is therefore a function both of stimulus strength and of applied regulators. There is a general positive correlation between time course and stimulus amplitude.

I next tested if the amplitude and time course of the response to a single pulse determines how successive pulses will build up. In Fig. 8 *F* the longer interpulse interval of 600 s gives rise to a larger response under basal conditions. In Fig. 8 *G* the regulator Gs is applied that makes the time course faster, and now the shorter interpulse interval of 180 s has the larger peak. Thus, changes in the response dynamics of feedback loops can lead to temporal tuning. For example, if downstream pathways act as peak detectors (e.g., they have sharp activation thresholds) then they will be tuned to interpulse intervals where the
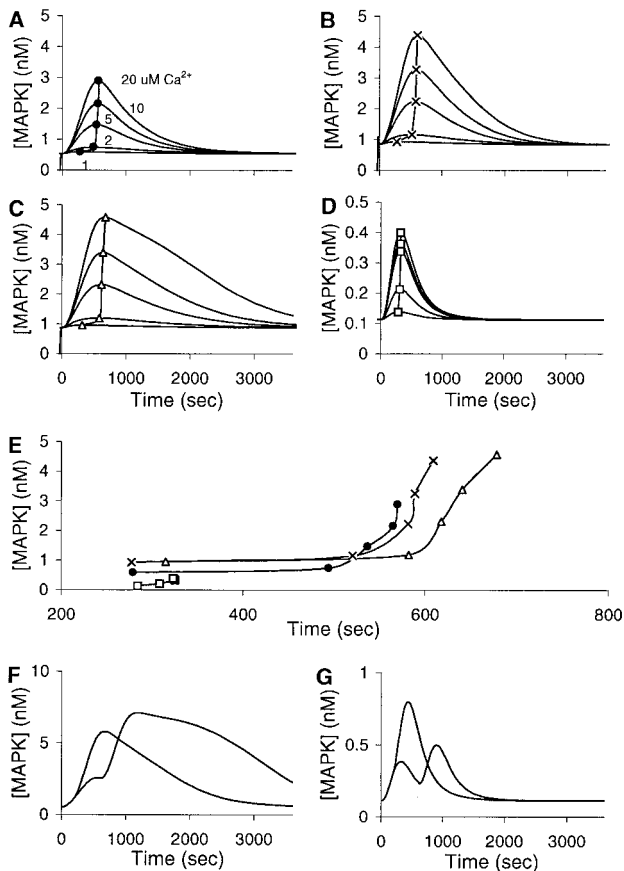
FIGURE 8 Subthreshold timing responses of the MAPK→PKC→PLA$_2$ feedback loop to a 1-s Ca^{2+} stimulus, under basal and three regulatory conditions and stimulus intensities from 1 to 20 μM Ca^{2+}. (*A*) Basal conditions. The time to the peak of the response increases with stimulus intensity. (*B*) Responses with 0.1 nM EGF stimulation. (*C*) Responses with 0.1 nM Glu stimulation. In addition to the increase in peak amplitude and timing, the width of the response is also wider. (*D*) Responses with 5 nM Gs regulation. Gs inhibits MAPK through the sequence Gs→AC→cAMP→PKA→Ras→MAPK. Note the reduced *y*-axis scale and the faster and narrower response. (*E*) Composite plot of peak timings at stimulus intensities of 1, 2, 5, 10, and 20 μM Ca^{2+}. Each regulator shifts both the peak amplitude and time, but the largest effect is due to Gs, which reduces both. (*F* and *G*) Summation of successive stimuli is a function of peak time and width. One-second Ca pulses at 16 μM are separated by 180 and 600 s in each panel. (*F*) Basal conditions. The 600-s peak is larger. (*G*) Regulation by 5-nM Gs. The 180-s peak is larger in this case.

peak response is maximal. Figs. 4 and 5 illustrate several examples of interpulse interval tuning where this mechanism may be important.

A similar series of Ca^{2+} stimuli (1, 2, 5, and 10 μM for 1 s) was applied to the CaMKII feedback loop. The activity of both the autophosphorylated, Ca^{2+}-autonomous form of CaMKII, as well as of the CaM-bound forms was compared. In contrast to the results for the MAPK loop, autonomous CaMKII responses shift to the left with increasing stimulus amplitude (Fig. 9 *A*). The regulatory effect of Gs is to
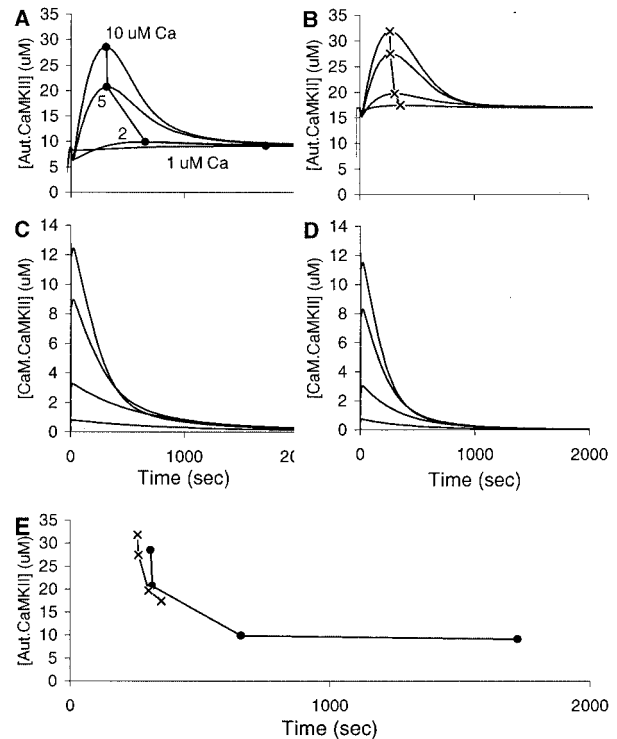

FIGURE 9 Responses of the CaMKII autophosphorylation feedback loop to 1-s Ca^{2+} stimulus of 1, 2, 5, and 10 μM. (*A*) Basal responses. As stimulus strength increases the time to peak decreases. (*B*) Responses in the presence of 1 nM Gs. The pathway Gs→AC→cAMP→PKA→PP1→CaMKII leads to a net increase in CaMKII activity. (*C*) Responses of CaM-activated CaMKII. The turn-on is almost immediate, but the time course of removal decreases slightly with increasing stimulus amplitude. (*D*) Responses of CaM-activated CaMKII in the presence of Gs. There is a slight decrease in available CaMKII because some of the kinase is basally phosphorylated. Otherwise the responses are not affected by the regulator. (*E*) Composite plot of time-courses for *A* and *B*. Response time decreases sharply as stimulus strength is increased from 1 μM Ca^{2+} to 10 μM Ca^{2+}. The decrease is less pronounced in the presence of basal Gs stimulation (×). At larger stimulus amplitudes the peak timing is not much affected by the presence of Gs.

increase CaMKII activity, and this further lowers the response time (Fig. 9 *B*). The CaM bound active forms of CaMKII have a very rapid activation time course, and the decay times decrease as the stimulus amplitude increases (Fig. 9 *C*). In this case Gs regulation has little effect (Fig. 9 *D*).

Overall, the simulations with the two feedback loops show that the response time course can be adjusted both by stimulus strength and by regulatory inputs. Interestingly, stronger stimuli increase the time course of the MAPK-PKC loop, whereas they decrease the time course for CaMKII. Thus feedback loops can also act as inputs (albeit with complex regulation) for weighted summation by downstream pathways.

DISCUSSION

Signaling networks are versatile computational machines. Their roles in processing information through summation,

integration, information storage, as logic elements, and as parts of the cellular machinery itself are all well documented (Alberts et al., 1994; Bray, 1995; Lauffenburger and Linderman, 1993; Roberson and Sweatt, 1999; Thron, 1997). This paper examines their role in temporal computation, and in particular in the operations of tuning and filtering in the intermediate time-scale, from around a second to an hour. More rapid events appear to be the domain of biophysical processes such as electrical signaling and calcium diffusion, and very slow events merge into the realm of genetics and cell biology. The kinds of temporal processing that may fall in the domain of signaling pathways include pattern recognition, storage of information (Sejnowski, 1999), and context-sensitive switching of tuning preference (Stanton, 1996). Signaling pathways in isolation are relatively uninteresting as timing devices as they typically have characteristic on and off response times to inputs. This paper examines how this simple timing behavior may scale into complex, and computationally relevant network timing properties. I report that: 1) there are two primary mechanisms for stimulus pattern decoding: weighted summation of signals from signaling pathways with different time-courses and alteration of dynamics of feedback loops; 2) regulators typically control timing in linear pathways by altering the amplitudes and baseline activity of pathways, rather than by altering the time course itself; and 3) both regulators and stimulus amplitude can change time-courses of feedback loops.

Mechanisms for stimulus tuning: weighted summation

Signaling pathways have characteristic time-courses, arising from the chemical rate constants of the individual reaction steps that comprise the pathway. A simple mechanism for tuning is weighted convergence of these characteristic responses onto downstream pathways. The output of this pathway will typically be a complex function of all the inputs, but to first order it can be thought of as a summation of the inputs with a different weight given to each input.

The first step in tuning may be a selection for inputs of different duration (Figs. 2 and 3). Two opposing effects shape these responses. First, the response tends to build up with increasing stimulus duration. Second, the stimulus amplitude itself declines in inverse proportion to the duration of the stimulus, when the total calcium flux is held constant. A variety of responses are observed as the stimulus duration increases (Fig. 2). Similar forms of tuning have previously been suggested in the completely different signaling context of bacterial chemotaxis (Bray, 1995).

The next step is the combination of such responses by convergence on downstream pathways. Wu et al. (2001a) report such a situation in hippocampal neurons where fast and slow pathways converge onto cyclic AMP response element-binding protein phosphorylation. Such composite

responses could give rise to interval tuning if the interpulse interval is the same as the time between successive phases of the response (Figs. 4 and 5). This form of tuning may have particular relevance for repetitive stimulus protocols used in studies on synaptic plasticity (Bliss and Collingridge, 1993). A number of experimental studies suggest that strong bursts of synaptic activity at an interval of 5 to 10 min may be particularly effective in activating the MAPK pathway (Wu et al., 2001b) and inducing synaptic potentiation (Blitzer et al., 1995; Winder et al., 1999). The simulations appear to match this interval. Several pathways in Fig. 4 have a peak in this time range, and the threshold for activating the MAPK-PLA$_2$-PKC feedback loop is lowest at 600 s (Fig. 5).

Three examples of response summation were considered in more detail by dissecting the signaling network into linear but converging cascades (Figs. 6 and 7). In each case it was possible to isolate the components of a complex downstream time course. Thus, the combined effects of duration filtering by individual pathways, and downstream weighted summation, can give rise to temporal tuning.

Mechanisms for stimulus tuning: feedback loops

The second mechanism of temporal tuning involves feedback loops. This is an expected outcome from analogy with electrical circuits (Horowitz and Hill, 1989). Numerous examples of complex temporal dynamics, including oscillations, have been reported for various kinds of positive and negative signaling feedback loops (Baier and Sahle, 1998; Kholodenko, 2000; Ngo and Roussel, 1997; Tang et al., 1996). A specific examination of the relationship between signaling time-courses and signal intensity was reported for a negative feedback loop in the MAPK system, using both experiments and simulations (Asthagiri and Lauffenburger, 2000). In the current paper, two positive feedback loops (MAPK-PLA$_2$-PKC and CaMKII autophosphorylation) were examined. Both exhibited a dependence of peak time and width on regulators and on the amplitude of the stimulus. Interestingly, increasing stimulus strength had opposite effects on peak time in the two cases (Figs. 8 and 9). The optimal interpulse-interval for summation of successive stimuli is related to the peak timing, and this is a function of regulatory inputs (Fig. 8, *F* and *G*). Combining these results with those previously reported (Asthagiri and Lauffenburger, 2000) it seems likely that feedback loops can be tuned to different combinations of intensity, duration, and interpulse interval. Tuning has also been reported for CaMKII autophosphorylation after repetitive Ca^{2+} pulses (Hanson et al., 1994).

What is the role of other emergent properties of feedback loops in temporal tuning? Two such properties are oscillations and bistability. These effects have been considered in detail in several other studies (Ferrell and Machleder, 1998; Kholodenko, 2000; Scheper et al., 1999; Thron, 1999).

Periodicity and its corollary of tuning to periodic stimuli are an outcome of oscillatory feedback (Ermentrout, 1994). Bistability has previously been shown to result in both long-term history effects as well as thresholding (Bhalla and Iyengar, 1999; Lisman, 1989). Long-term switching of tuning properties could be one outcome of bistability. In the current study the phenomenon of thresholding is used as a measure of integrated network response and to illustrate how temporal tuning could give rise to network selectivity between input patterns.

Regulation of stimulus tuning

The current simulations illustrate some possible mechanisms for regulation of temporal tuning by signaling pathways. The obvious mechanism would be for the regulator to directly change the time course of one or more inputs. For example, it might seem plausible that a steady regulatory input might alter the rate of production of a second messenger and thereby alter its time course. Unexpectedly, none of the regulatory inputs tested in this study functioned in this manner. Instead, tuning changes appear to occur due to changes in baseline and "gain" of inputs with different timings (Figs. 6 and 7). Downstream responses become dominated by the time course of the signal whose amplitude has been boosted by the regulator. In effect, the regulators appear to alter the weights of converging inputs with different time-courses.

A second mechanism for tuning regulation operates on feedback loops. This is more difficult to dissect out because such loops are inherently nonlinear. Several such analyses have previously been carried out (Baier and Sahle, 1998; Ermentrout, 1994). Even in the subthreshold and nonoscillatory regime of the current analysis, there were clear shifts in time course of response due to the presence of regulatory inputs (Figs. 8 and 9).

Interpretation and caveats

These simulations are at an early phase of quantitative model building, so there are gaps in the roster of signaling pathways, and abstractions with regard to spatial and genetic interactions. Thus, the observed tuning mechanisms are probably a subset of those present in nature. The temporal domain of this model is in a window of a few seconds to approximately an hour, excluding both the detailed calcium dynamics and biophysics that underlies synaptic enhancement due to coincidence in pre- and postsynaptic spike timings (Markram et al., 1997) and late events in long-term potentiation (Frey and Morris, 1998). To the extent that the current pathways and mass-action kinetics represent a common denominator of far more complex signaling events, it seems plausible that the mechanisms
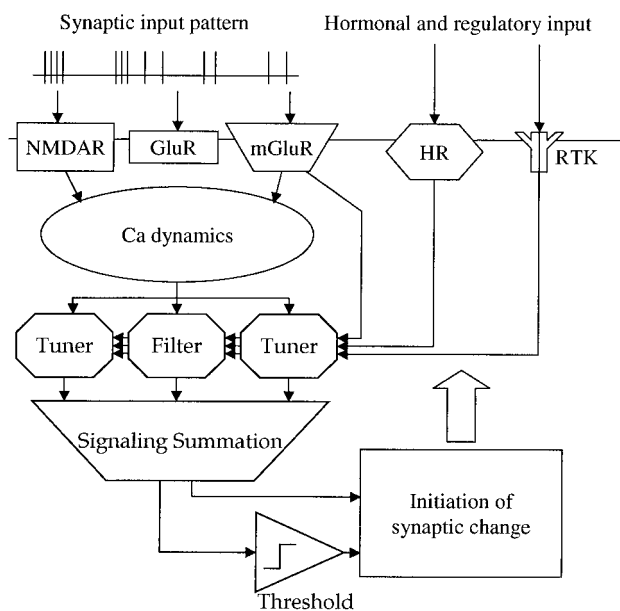

FIGURE 10 Schematic for temporal tuning by synaptic signaling pathways. Temporally patterned synaptic input is integrated by cellular biophysical processes and Ca^{2+} dynamics to give patterned Ca^{2+} signals. The network of signaling pathways acts as a bank of filters and tuners, each with a distinctive time course. The weight of each of these tuning processes is altered by various regulatory inputs. The temporally filtered signals are then summed by downstream pathways. Further signaling events such as thresholding and initiation of synaptic change eventually feed back to the inputs and the signaling network.

discussed here may underlie more sophisticated forms of temporal tuning in biological signaling networks.

One of the major limitations of mass-action models arises from the reliance on test-tube chemical data. Despite this limitation, such parameters are valuable in capturing some of the key interactions in the relevant range of time-scales, and in prediction of likely signaling mechanisms that form the basis for interesting cellular events. This study suggests a possible abstraction of synaptic signaling (Fig. 10). The signaling network could be represented as a bank of temporal filters and tuning elements with different time-courses, in series with thresholding and bistable elements, feeding into downstream effector processes. There is already considerable evidence that the selection between different forms of synaptic change is not just a function of stimulus intensity and that stimulus pattern also plays a critical role (Abbott and Nelson, 2000; Fields et al., 1997; Grover and Teyler, 1990). The current study approaches the system from a bottom-up description of rate constants and chemistry, and suggests that the same conclusion could be drawn from completely different premises.

This paper identifies an unexpectedly simple mechanism for temporal tuning based on weighted convergence of inputs from pathways with different time-courses. Tuning changes appear to involve changes in the weights for dif-

ferently timed inputs, rather than changing time-courses of elements in the same circuit. Feedback-loops exhibit somewhat more complex temporal filtering properties and can also act as tuned inputs converging onto downstream pathways. These mechanistic principles for signaling network tuning may suggest target points for regulation and provide a useful abstraction for thinking about temporal response properties of signaling networks.

REFERENCES

Abbott, L. F., and S. B. Nelson. 2000. Synaptic plasticity: taming the beast. *Nat. Neurosci.* 3:1178–1183.

Alberts, B., D. Bray, J. Lewis, M. Raff, K. Roberts, and J. D. Watson. 1994. Molecular Biology of the Cell. Garland Publishing Inc., New York.

Asthagiri, A. R., and D. A. Lauffenburger. 2000. Bioengineering models of cell signaling. *Annu. Rev. Biomed. Eng.* 2:31–53.

Baier, G., and S. Sahle. 1998. Homogeneous and spatio-temporal chaos in biochemical reactions with feedback inhibition. *J. Theor. Biol.* 193: 233–242.

Barr, D. S., N. A. Lambert, K. L. Hoyt, S. D. Moore, and W. A. Wilson. 1995. Induction and reversal of long-term potentiation by low- and high-intensity theta pattern stimulation. *J. Neurosci.* 15:5402–5410.

Bhalla, U. S. 1998. The network within: signaling pathways. *In* The Book of GENESIS: Exploring Realistic Neural Models with the GEneral NEural SImulation System. J.M. Bower and D. Beeman, editors. Springer-Verlag, New York. 169–190.

Bhalla, U. S., and R. Iyengar. 1999. Emergent properties of networks of biological signaling pathways. *Science.* 283:381–387.

Bhalla, U. S., and R. Iyengar. 2001. Robustness of the bistable behavior of a biological signaling feedback loop. *Chaos.* 11:221–226.

Bliss, T. V. P., and G. L. Collingridge. 1993. A synaptic model of memory: long-term potentiation in the hippocampus. *Nature.* 361:31–39.

Blitzer, R. D., T. Wong, R. Nouranifar, R. Iyengar, and E. M. Landau. 1995. Postsynaptic cAMP pathway gates early LTP in hippocampal CA1 region. *Neuron.* 15:1–20.

Bray, D. 1995. Protein molecules as computational elements in living cells. *Nature.* 376:307–312.

Ermentrout, G. B. 1994. The mathematics of biological oscillators. *Methods Enzymol.* 240:198–216.

Ferrell, J. E., Jr., and E. M. Machleder. 1998. The biochemical basis of an all-or-none cell fate switch in *Xenopus* oocytes. *Science.* 280:895–898.

Fields, R. D., F. Eshete, B. Stevens, and K. Itoh. 1997. Action potential-dependent regulation of gene expression: temporal specificity in Ca^{2+}, cAMP-responsive element binding proteins, and mitogen-activated protein kinase signaling. *J. Neurosci.* 17:7252–7266.

Frey, U., and R. G. Morris. 1998. Synaptic tagging: implications for late maintenance of hippocampal long-term potentiation. *Trends Neurosci.* 21:181–188.

Grover, L. M., and T. J. Teyler. 1990. Two components of long-term potentiation induced by different patterns of afferent activation. *Nature.* 347:477–479.

Hanson, P. I., T. Meyer, L. Stryer, and H. Schulman. 1994. Dual role of calmodulin in autophosphorylation of multifunctional CaM kinase may underlie decoding of calcium signals. *Neuron.* 12:943–956.

Horowitz, P., and W. Hill. 1989. The Art of Electronics. Cambridge University Press, Cambridge, UK.

Kholodenko, B. N. 2000. Negative feedback and ultrasensitivity can bring about oscillations in the mitogen-activated protein kinase cascades. *Eur. J. Biochem.* 267:1583–1588.

Lauffenburger, D. A., and J. J. Linderman. 1993. Receptors: models for binding, trafficking and signaling. Oxford University Press, Oxford, UK.

Levchenko, A., J. Bruck, and P. W. Sternberg. 2000. Scaffold proteins may biphasically affect the levels of mitogen-activated protein kinase signaling and reduce its threshold properties. *Proc. Natl. Acad. Sci. U. S. A.* 97:5818–5823.

Lisman, J. 1989. A mechanism for the Hebb and the anti-Hebb processes underlying learning and memory. *Proc. Natl. Acad. Sci. U. S. A.* 86: 9574–9578.

Lisman, J. 1994. The CaM kinase II hypothesis for the storage of synaptic memory. *Trends Neurosci.* 17:406–412.

Lu, W., H. Man, W. Ju, W. S. Trimble, J. F. MacDonald, and Y. T. Wang. 2001. Activation of synaptic NMDA receptors induces membrane insertion of new AMPA receptors and LTP in cultured hippocampal neurons. *Neuron.* 29:243–254.

MacGregor, R. J. 1987. Neural and brain modeling. Academic Press, San Diego, CA.

Markram, H., J. Lubke, M. Frotscher, and B. Sakmann. 1997. Regulation of synaptic efficacy by coincidence of postsynaptic APs and EPSPs. *Science.* 275:213–215.

Meyer, T., P. I. Hanson, L. Stryer, and H. Schulman. 1992. Calmodulin trapping by calcium-calmodulin-dependent protein kinase. *Science.* 256: 1199–2021.

Ngo, L. G., and M. R. Roussel. 1997. A new class of biochemical oscillator models based on competitive binding. *Eur. J. Biochem.* 245:182–190.

Nguyen, P. V., S. N. Duffy, and J. Z. Young. 2000. Differential maintenance and frequency-dependent tuning of LTP at hippocampal synapses of specific strains of inbred mice. *J. Neurophysiol.* 84:2484–2493.

Roberson, E. D., and J. D. Sweatt. 1999. A biochemical blueprint for long-term memory. *Learn Mem.* 6:381–388.

Scheper, T. O., D. Klinkenberg, J. van Pelt, and C. Pennartz. 1999. A model of molecular circadian clocks: multiple mechanisms for phase shifting and a requirement for strong nonlinear interactions. *J. Biol. Rhythms.* 14:213–220.

Sejnowski, T. J. 1999. The book of hebb. *Neuron.* 24:773–776.

Shimizu, T. S., N. Le Novere, M. D. Levin, A. J. Beavil, B. J. Sutton, and D. Bray. 2000. Molecular model of a lattice of signalling proteins involved in bacterial chemotaxis. *Nat. Cell Biol.* 2:E199–E201.

Soderling, T. R., and V. A. Derkach. 2000. Postsynaptic protein phosphorylation and LTP. *Trends Neurosci.* 23:75–80.

Stanton, P. K. 1996. LTD, LTP, and the sliding threshold for long-term synaptic plasticity. *Hippocampus.* 6:35–42.

Svoboda, K., D. W. Tank, and W. Denk. 1996. Direct measurement of coupling between dendritic spines and shafts. *Science.* 272:716–719.

Tang, Y., J. L. Stephenson, and H. G. Othmer. 1996. Simplification and analysis of models of calcium dynamics based on IP3-sensitive calcium channel kinetics. *Biophys. J.* 70:246–263.

Thron, C. D. 1997. Bistable biochemical switching and the control of the events of the cell cycle. *Oncogene.* 15:317–325.

Thron, C. D. 1999. Mathematical analysis of binary activation of a cell cycle kinase which down-regulates its own inhibitor. *Biophys. Chem.* 79:95–106.

Winder, D. G., K. C. Martin, I. A. Muzzio, D. Rohrer, A. Chruscinski, B. Kobilka, and E. R. Kandel. 1999. ERK plays a regulatory role in induction of LTP by theta frequency stimulation and its modulation by beta-adrenergic receptors. *Neuron.* 24:715–726.

Wu, G.-Y., K. Deisseroth, and R. W. Tsien. 2001a. Activity-dependent CREB phosphorylation: convergence of a fast, sensitive calmodulin kinase pathway and a slow, less sensitive mitogen-activated protein kinase pathway. *Proc. Natl. Acad. Sci. U. S. A.* 98:2808–2813.

Wu, G.-Y., K. Deisseroth, and R. W. Tsien. 2001b. Spaced stimuli stabilize MAPK pathway activation and its effects on dendritic morphology. *Nat. Neurosci.* 4:151–158.